MRI for Parathyroid Imaging

Kambiz Nael, M.D.

Department of Radiology, Mount Sinai Hospital, New York, NY, USA

Background

Primary hyperparathyroidism (PHPT) is a common cause of hypercalcemia, with an estimated incidence of approximately 25 to 30 cases per 100,000 people. Approximately 85 to 90% of these cases are caused by single parathyroid adenomas (PTA), while multiglandular disease and parathyroid hyperplasia account for the remainder of cases with PHPT [1].

Diagnosis is often made by biochemical tests (serum Ca^{++} and PTH) in an appropriate clinical setting. Definitive treatment requires surgical excision, and preoperative localization with imaging is used to minimize the extent of surgery and complication rates [2].

Traditionally, ultrasound and Technetium-99m (^{99m}Tc) Sestamibi scintigraphy have been used as first line tools to localize parathyroid adenomas. Ultrasound takes advantage of differential echogenicity of PTA compared to thyroid tissue, and scintigraphy takes advantage of physiologically differences in radiopharmaceutical uptake and retention. These tests can often be inconclusive, which has led to the development of other cross-sectional imaging such as dynamic multiphasic CT (4D CT) or dynamic MRI (Fig. 1).

Key points:

1. The MR technique described below has significantly improved on the traditional drawbacks of MR for parathyroid imaging including limited spatial and temporal resolution.
2. Four-dimensional (4D) contrast-enhanced MRI with high spatial and temporal resolution can be obtained for evaluation of parathyroid adenomas and has the potential to be used as a strong alternative imaging modality to Technetium (^{99m}Tc) Sestamibi or 4D CT without the need for radiation.
3. Multiparametric quantitative MR perfusion analysis can be used to distinguish parathyroid adenomas from subjacent thyroid tissue or lymph nodes.

Implications for patient care:

In patients with primary hyperparathyroidism, the described 4D DCE MRI technique provides additional means to accurately identify and characterize parathyroid adenomas without the need of radiation required for alternative imaging such as 4D CT or ^{99m}Tc-Sestamibi scan.

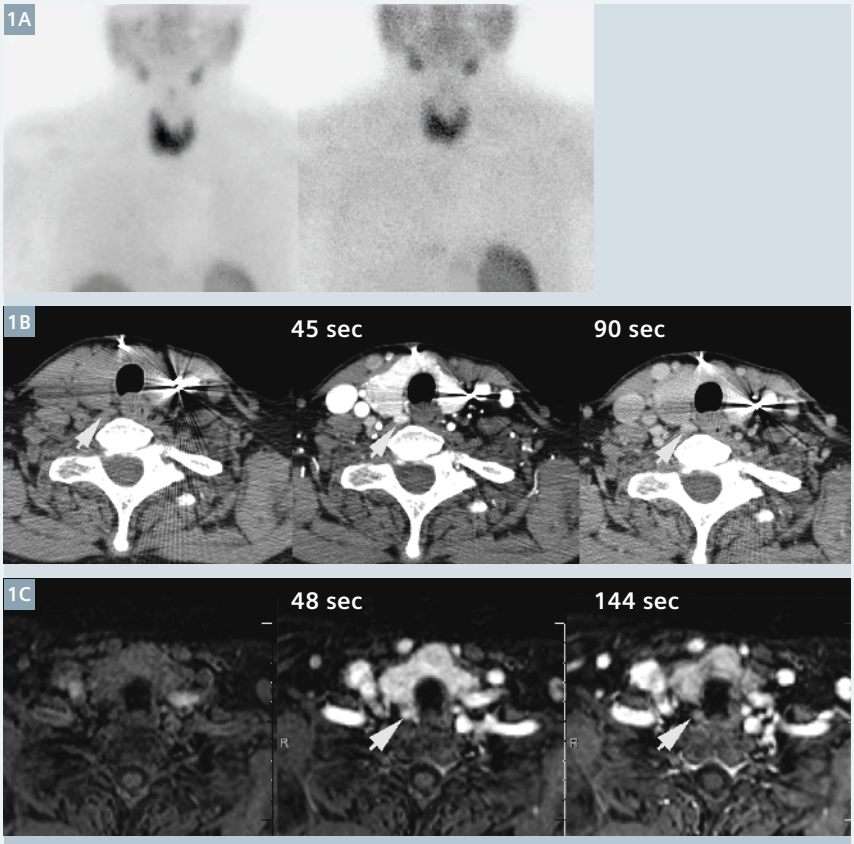

1 71-year-old woman with primary hyperparathyroidism (PHPT), who had left-sided parathyroidecotomy 3 years ago (note surgical clips on CT); now presenting with recurrent PHPT (PTH: 120 pg/mL, Ca^{++}: 10.6 mg/dL). **(1A)**: Tc-Sestamibi scan is negative. **(1B)**: 3-phase dynamic CT images including un-enhanced, arterial phase (45 sec) and venous phase (90 sec) images are shown, demonstrating a 5 mm arterial enhancing nodule (arrows) in the right tracheoesophegeal groove just posterior to the right thyroid lobe which shows washout on delayed phase. **(1C)**: Selected axial multiframe MR images from dynamic contrast-enhanced MR sequence are shown, demonstrating arterial enhancing PTA (arrows) that shows significant washout on delayed venous phase.

The main target of these cross-sectional studies is to exploit hypervascular nature of PTAs, a principle that was established in 1970s by the use of arterial catheter angiography [3, 4]. 4D CT has shown superior accuracy compared to scintigraphy [5] and has shown significant promise for identification and characterization of PTAs [6-8]. However there are two lingering problems associated with 4D CT:

1. Since continuous CT acquisition during the entire dynamic course of contrast through parathyroid glands is prohibited by the radiation dose, 4D CT provides only snapshots of contrast dynamic at certain time points (depending on the number of acquisitions). There are a variety of acquisition schemes using a combination of unenhanced and multiple post-contrast phases including 2 phases [9, 10], 2.5 phases [11, 12], 3 phases [8, 13] or 4 phases [14-17] with time interval ranging from 30 to 90 sec, each with strengths and limitations. However there is no consensus on the number and time-interval between CT acquisitions for an optimal 4D CT.
2. Radiation dose remains the main inherent disadvantage of CT. Despite using dose reduction techniques, effective radiation dose delivered by 4D CT ranges from 5.56 to 10.4 mSv [8, 18, 19] depending on the acquisition scheme used.

For these reasons, there remains a role for MRI to be explored in parathyroid imaging.

MRI technical considerations

MRI is an attractive alternative to both scintigraphy and 4D CT due to lack of radiation and has been used for the evaluation of PTAs with some success [20-22], though not with the same effectiveness as 4D CT. Fast image acquisition and high spatial resolution have long been significant advantages of CT and hence significant attention has been given to 4D CT for the detection of PTAs. Traditional technical limitations to localizing PTAs with MR have recently been addressed with modern MR technology. These include:

3. Limited spatial and temporal resolution for multiphase dynamic contrast enhanced (DCE) MR imaging over a large field-of-view required for parathyroid imaging. This limitation can be addressed by the use of fast imaging tools such as time-resolved angiography with stochastic trajectories (TWIST) [23] and improved parallel imaging technique such as Controlled Aliasing in Parallel Imaging Results in Higher Acceleration (CAIPIRINHA) [24].
4. Inhomogeneity of fat-suppression in the neck that is required for the detection of small parathyroid adenomas. Dixon fat-suppression technique [25] can significantly improve this shortcoming [26].

In our institution, using a modified MR sequence that incorporates Dixon fat saturation technique and fast imaging tools such as TWIST and CAIPIRINHA, we have established a 4D dynamic MRI protocol for the accurate identification and characterization of PTAs [27, 28].

How we do it?

Image acquisition

In order to offset signal-to-noise (SNR) penalty associated with fast imaging tools such as TWIST and CAIPIRINHA, we use 3T MRI for our parathyroid imaging (MAGNETOM Skyra MRI system, Siemens Healthcare, Erlangen, Germany). A combination of 20-element head and neck coil is used for radiofrequency signal reception. Our MR imaging protocol includes axial T2w Fat sat, coronal STIR, coronal T1w pre contrast and 4D dynamic contrast-enhanced (DCE) sequences. 4D-DCE imaging is performed using a 3D VIBE (volumetric interpolated examination) sequence with the following parameters: (TR: 4.06 ms, 1st TE: 1.31 ms, 2nd TE: 2.54 ms, FA: 9°, matrix: 160 mm, FOV: 200 mm, 60 slices x 2 mm thick). The TWIST VIBE and Dixon fat/water separation are merged into one pulse sequence [29]. Bipolar readout gradients are used to produce two partial echoes at a first (TE: 1.31 ms) and a second (TE: 2.54 ms) echo time. Bipolar gradients allow for a shorter TR (4.6 ms) as well as less echo asymmetry. Integration of TWIST as an echo-sharing technique with sampling density of 33% results in x2 acceleration. In addition, CAIPIRINHA with accel-eration factor of 4 is incorporated, to increase net acceleration to a factor of 8.

Using these combinations we acquire a 3D data set with voxel size of 1.3 x 1.3 x 2 mm^3 and temporal resolution of 6 seconds over a cranio-caudal coverage of 120 mm. This coverage is adequate to encompass from the inferior mandibular rim to the carina in most patients. We acquire 24 temporal frames for a total of 140 sec acquisition time. Four of these temporal frames (about 25 sec) are acquired before contrast injection to establish the baseline required for DCE analysis. A total of 0.1 mmol/kg of gadolinium is injected at 4 ml/sec.

Image analysis

Identification: For pre-operative localization, T2w fat-sat and 4D dynamic series are most scrutinized. The majority of PTAs are T2 hyperintense and should demonstrate early arterial enhancement (Fig. 2). Having high-spatial resolution voxels (1.3 x 1.3 x 2 mm^3) over a craniocaudal diameter of 12 cm (from mandibular rim to manubrium) allow for accurate examination of both native and ectopic adenomas as small as 3 mm. Having this data set every 6 seconds provides a true 4D capability for interrogation of contrast-enhancement cure of PTA over the course of image acquisition (144 sec). In contrast to 4D CT in which the number of acquisitions (ranging from 2 to 4) is limited by the prohibitive effect of radiation dose, using our 4D DCE MR, 24 time frames are acquired every 6 seconds to truly exploit the hypervascular nature of these lesions. This takes out the guesswork that is required in using 4D CT to capture the arterial phase. In our experience the majority of these PTAs are enhancing at the same time as, or one temporal frame before, the enhancement of thyroid bed (Fig. 2). The peak-enhancement of PTAs are often 6 to 12 seconds (1 to 2 temporal frames) before the peak-enhancement

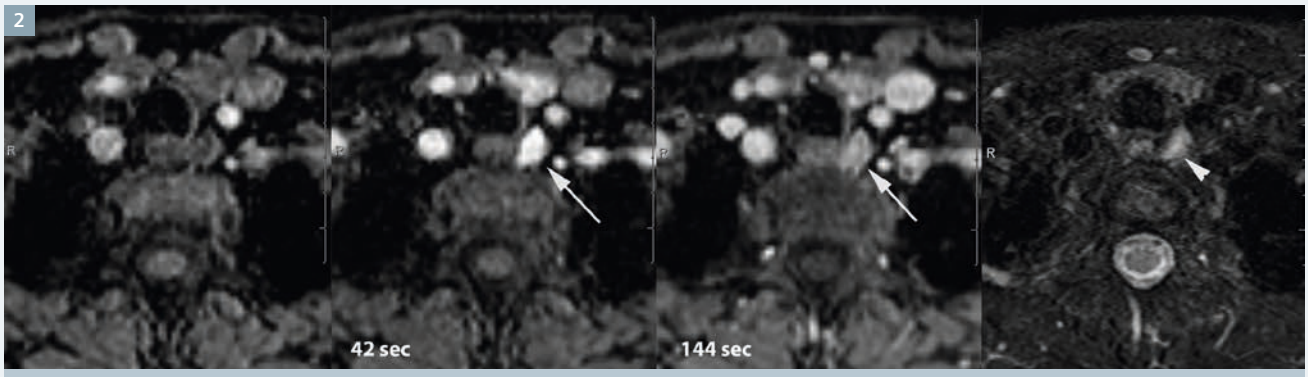

2 55-year-old woman, with serum Ca^{++} of 12.2 and advanced osteoporosis as the result of her primary hyperparathyroidism (PHPT). Selected axial multiframe MR images from dynamic contrast-enhanced MR sequence are shown, demonstrating arterial enhancing PTA 42 seconds after contrast injection (arrows). This lesion is hyperintense on T2w images (arrowhead), which shows significant wash-out (40%) during later venous phase at 144 seconds post contrast injection.

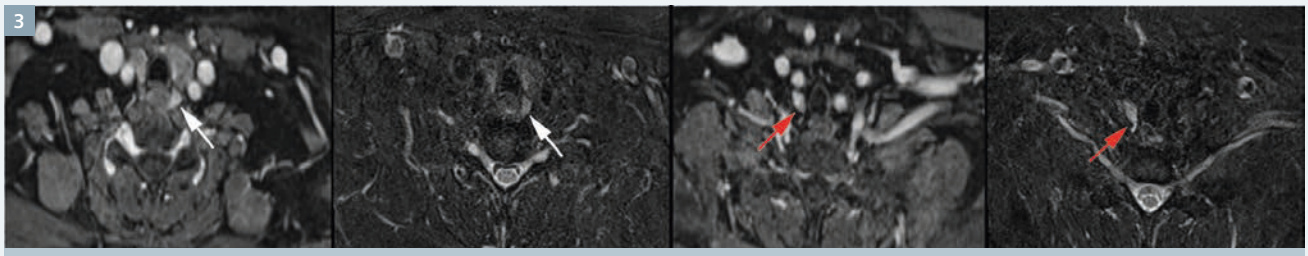

3 68-year-old woman primary hyperparathyroidism (PHPT) who was found to have multiglandular disease involving all four parathyroid glands on pre-operative MRI, confirmed by surgical pathology. Selected axial images from 4D dynamic-contrast-enhanced series and corresponding T2w images show enlarged T2 hyperintense enhancing nodules of the left lower gland (white arrows) and right lower gland (red arrows) indicative of adenomatous enlargement seen with multiglandular hyperplasia. Note the excellent image quality of the 4D dynamic series that are obtained with voxel size of 1.3 x 1.3 x 2 mm^3 every 6 seconds. Also homogenous fat-saturation is achieved by using Dixon fat-saturation technique.

of the thyroid gland. In our experience, having a T2 hyperintense arterial enhancing nodule in the native parathyroid gland space or along the expected embryologic course of parathyroid glands such as tracheo-esophageal groove or superior mediastinum is extremely likely to be a PTA. Our preliminary data for pre-operative detection of PTA has shown a sensitivity close to 100% and positive-predictive value close to 1 for single PTA, while sensitivity drops to between 64 and 75% for multiglandular disease (Fig. 3) [28].

Characterization: The dynamic information inherent to this 4D DCE data set can be used to characterize PTA and differentiate them from PTA mimics such as cervical lymph nodes or subjacent thyroid tissue. This is particularly useful when you have a few PTA candidate lesions to narrow the differential diagnosis and provide the surgeon with the most likely lesion to be a true PTA [27] (Fig. 4).

The perfusion datasets are processed using commercially available FDA approved software (Olea Sphere, Olea Medical SAS, La Ciotat, France). Multiparametric quantitative perfusion parameters including peak enhancement, time-to-peak (TTP), wash-in and wash-out can be computed from the concentration-time curve. Multiparametric perfusion biomarkers can successfully exploit the hypervascular nature of PTAs, a feature that can be used to differentiate them from subjacent cervical lymph node and thyroid tissue. In our experience, TTP and wash-in, two characteristics of arterial enhancement, are significantly different in PTAs vs. cervical lymph nodes and thyroid tissue (Fig. 4). PTAs show significantly faster arterial enhancement with a mean TTP enhancement of 13 and 29 seconds earlier than thyroid tissue and normal cervical lymph node respectively. In addition the wash-in and wash-out values are significantly higher in PTAs. Using multiparametric MR perfusion and combined ROC analysis, the best overall model to distinguish PTA from cervical lymph node consists of a combination of TTP, wash-in and wash-out yielding an AUC of 0.96, superior to any individual or combination of other classifiers [27].

Conclusion

Dynamic 4D contrast-enhanced MRI with high temporal and spatial resolutions can now be obtained for pre-operative identification of PTAs, providing a strong alternative imaging modality to 4D CT without the need for radiation. Multiparametric MR perfusion can be used to exploit the hypervascular nature of PTAs to distinguish them from subjacent thyroid tissue or lymph nodes with high accuracy.

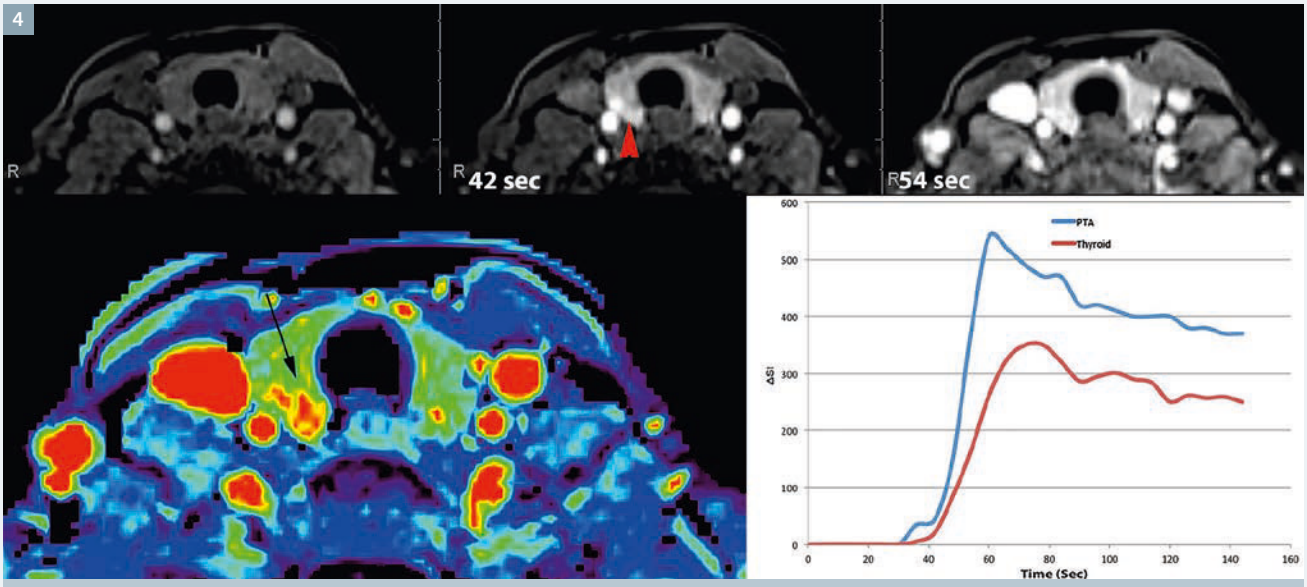

4 61-year-old woman with primary hyperparathyroidism (PTH: 118 pg/mL, Ca^{++}: 10.9 mg/dL) Note differential contrast enhancement of a small nodule in the posterior lobe of the right thyroid gland (red arrowhead) during the arterial phase 42 second after contrast injection and corresponding increased peak enhancement (arrow) on perfusion map in this surgically proven intrathyroid PTA. Note that on two imaging frames latter (54 sec), the nodule is less conspicuous due to increasing enhancement of the thyroid tissue. Contrast-time curve analysis from ROIs placed over the PTA and thyroid gland shows significantly faster and higher peak enhancement and higher wash-in and significant washout values in PTA in comparison to the thyroid gland.

Acknowledgement

I like to thank Kevin J. Johnson (Clinical Applications Scientist, Siemens Medical Solutions USA, Inc.) for his help and contribution for imaging protocol adjustment.

References

1 Heath H, 3rd, Hodgson SF, Kennedy MA. Primary hyperparathyroidism. Incidence, morbidity, and potential economic impact in a community. The New England journal of medicine. Jan 24 1980;302(4):189-193.
2 Chen H, Mack E, Starling JR. A comprehensive evaluation of perioperative adjuncts during minimally invasive parathyroidectomy: which is most reliable? Annals of surgery. Sep 2005; 242(3):375-380; discussion 380-373.
3 Doppman JL. Parathyroid localization: arteriography and venous sampling. Radiologic clinics of North America. Aug 1976;14(2):163-188.
4 Miller DL, Doppman JL. Parathyroid angiography. Annals of internal medicine. Dec 1987;107(6):942-943.
5 Mortenson MM, Evans DB, Lee JE, et al. Parathyroid exploration in the reoperative neck: improved preoperative localization with 4D-computed tomography. Journal of the American College of Surgeons. May 2008;206(5):888-895; discussion 895-886.
6 Day KM, Elsayed M, Beland MD, Monchik JM. The utility of 4-dimensional computed tomography for preoperative localization of primary hyperparathyroidism in patients not localized by sestamibi or ultrasonography. Surgery. Mar 2015;157(3):534-539.
7 Cham S, Sepahdari AR, Hall KE, Yeh MW, Harari A. Dynamic Parathyroid Computed Tomography (4DCT) Facilitates Reoperative Parathyroidectomy and Enables Cure of Missed Hyperplasia. Annals of surgical oncology. Feb 18 2015.
8 Kelly HR, Hamberg LM, Hunter GJ. 4D-CT for preoperative localization of abnormal parathyroid glands in patients with hyperparathyroidism: accuracy and ability to stratify patients by unilateral versus bilateral disease in surgery-naive and re-exploration patients. AJNR Am J Neuroradiol. Jan 2014;35(1):176-181.
9 Linda DD, Ng B, Rebello R, Harish S, Ioannidis G, Young JE. The utility of multidetector computed tomography for detection of parathyroid disease in the setting of primary hyperparathyroidism. Canadian Association of Radiologists journal = Journal l'Association canadienne des radiologistes. May 2012;63(2):100-108.
10 Gafton AR, Glastonbury CM, Eastwood JD, Hoang JK. Parathyroid lesions: characterization with dual-phase arterial and venous enhanced CT of the neck. AJNR Am J Neuroradiol. May 2012;33(5):949-952.
11 Kutler DI, Moquete R, Kazam E, Kuhel WI. Parathyroid localization with modified 4D-computed tomography and ultrasonography for patients with primary hyperparathyroidism. The Laryngoscope. Jun 2011;121(6):1219-1224.
12 Harari A, Zarnegar R, Lee J, Kazam E, Inabnet WB, 3rd, Fahey TJ, 3rd. Computed tomography can guide focused exploration in select patients with primary hyperparathyroidism and negative sestamibi scanning. Surgery. Dec 2008; 144(6):970-976; discussion 976-979.
13 Chazen JL, Gupta A, Dunning A, Phillips CD. Diagnostic accuracy of 4D-CT for parathyroid adenomas and hyperplasia. AJNR Am J Neuroradiol. Mar 2012; 33(3):429-433.
14 Starker LF, Mahajan A, Bjorklund P, Sze G, Udelsman R, Carling T. 4D parathyroid CT as the initial localization study for patients with de novo primary hyperparathyroidism. Annals of surgical oncology. Jun 2011;18(6):1723-1728.
15 Beland MD, Mayo-Smith WW, Grand DJ, Machan JT, Monchik JM. Dynamic MDCT for localization of occult parathyroid adenomas in 26 patients with primary hyperparathyroidism. AJR. American journal of roentgenology. Jan 2011;196(1):61-65.
16 Rodgers SE, Hunter GJ, Hamberg LM, et al. Improved preoperative planning for directed parathyroidectomy with 4-dimensional computed tomography. Surgery. Dec 2006;140(6):932-940; discussion 940-931.
17 Hunter GJ, Schellingerhout D, Vu TH, Perrier ND, Hamberg LM. Accuracy of four-dimensional CT for the localization of

abnormal parathyroid glands in patients with primary hyperparathyroidism. Radiology. Sep 2012;264(3):789-795.
18 Mahajan A, Starker LF, Ghita M, Udelsman R, Brink JA, Carling T. Parathyroid four-dimensional computed tomography: evaluation of radiation dose exposure during preoperative localization of parathyroid tumors in primary hyperparathyroidism. World journal of surgery. Jun 2012;36(6):1335-1339.
19 Madorin CA, Owen R, Coakley B, et al. Comparison of radiation exposure and cost between dynamic computed tomography and sestamibi scintigraphy for preoperative localization of parathyroid lesions. JAMA surgery. Jun 2013; 148(6):500-503.
20 Gotway MB, Reddy GP, Webb WR, Morita ET, Clark OH, Higgins CB. Comparison between MR imaging and 99mTc MIBI scintigraphy in the evaluation of recurrent of persistent hyperparathyroidism. Radiology. Mar 2001;218(3):783-790.
21 Lee VS, Spritzer CE, Coleman RE, Wilkinson RH, Jr., Coogan AC, Leight GS, Jr. The complementary roles of fast spin-echo MR imaging and double-phase 99m Tc-sestamibi scintigraphy for localization of hyperfunctioning parathyroid glands. AJR. American journal of roentgenology. Dec 1996;167(6):1555-1562.
22 Grayev AM, Gentry LR, Hartman MJ, Chen H, Perlman SB, Reeder SB. Presurgical localization of parathyroid adenomas with magnetic resonance imaging at 3.0 T: an adjunct method to supplement traditional imaging. Annals of surgical oncology. Mar 2012;19(3):981-989.
23 Song T, Laine AF, Chen Q, et al. Optimal k-space sampling for dynamic contrast-enhanced MRI with an application to MR renography. Magnetic resonance in medicine: official journal of the Society of Magnetic Resonance in Medicine / Society of Magnetic Resonance in Medicine. May 2009;61(5):1242-1248.
24 Breuer FA, Blaimer M, Heidemann RM, Mueller MF, Griswold MA, Jakob PM. Controlled aliasing in parallel imaging results in higher acceleration (CAIPIRINHA) for multi-slice imaging. Magnetic resonance in medicine : official journal of the Society of Magnetic Resonance in Medicine / Society of Magnetic Resonance in Medicine. Mar 2005;53(3):684-691.
25 Dixon WT. Simple proton spectroscopic imaging. Radiology. Oct 1984; 153(1):189-194.
26 Barger AV, DeLone DR, Bernstein MA, Welker KM. Fat signal suppression in head and neck imaging using fast spin-echo-IDEAL technique. AJNR Am J Neuroradiol. Jun-Jul 2006;27(6):1292-1294.
27 Nael K, Hur S.H, Bauer A, Khan R, Guerrero M. Multiparametric MR Perfusion in Characterization of Parathyroid Adenomas. Paper presented at: ASNR 53rd Annual Meeting; Apr 28, 2015; Chicago, IL.
28 Khan R Hur S.H, Guerrero M, Inampudi R, Nael K. 4D MRI at 3T to Preoperatively detect Single Parathyroid Adenoma and Multi-glandular Disease: A Feasibility Study. Paper presented at: ASNR 53rd Annual Meeting; Apr 28, 2015; Chicago, IL.
29 Le Y, Kroeker R, Kipfer HD, Lin C. Development and evaluation of TWIST Dixon for dynamic contrast-enhanced (DCE) MRI with improved acquisition efficiency and fat suppression. J Magn Reson Imaging. Aug 2012;36(2):483-491.

Contact

Kambiz Nael, M.D.
Assistant Professor of Radiology
Department of Radiology
Mount Sinai Hospital
1176 5th Avenue, Box 1235
New York, NY 10029, USA
kambiznael@gmail.com